This article has been accepted for publication in a future issue of this journal, but has not been fully edited. Content may change prior to final publication. Citation information: DOI 10.1109/TAP.2019.2918443, IEEE Transactions on Antennas and Propagation

EMSIW based Compact High Gain Wide Full Space Scanning LWA with Improved Broadside Radiation Profile

Anirban Sarkar, *Student Member, IEEE*, Abhishek Sharma, *Student Member, IEEE*, Animesh Biswas, *Senior Member, IEEE*, and M. J. Akhtar, *Senior Member, IEEE*

***Abstract*—A novel compact high gain eighth-mode substrate integrated waveguide (EMSIW) based double asymmetry (DA) composite right/left handed (CRLH) leaky-wave antenna with larger degrees of freedom to control the efficiency is proposed and investigated. The proposed tilted DA radiating EMSIW incorporated with radiating interdigital capacitive (IDC) slots enable the unit cell to hold CRLH property with improved compactness and gain. The DA not only provides increased efficiency at broadside frequency than off-broadside but also offers more degrees of freedom to independently control the series and shunt resonators of the proposed geometry. Dispersion analysis is done by full wave simulation and validated by theoretical analysis through predicted equivalent circuit model for achieving the balance condition of unit cell which facilitates the complete elimination of open-stopband. Due to the systematic placement of interdigital slots on radiating EMSIW unit cell, the radiation intensity profile is significantly enhanced which leads to higher directivity and notable enhanced gain (17.96 dBi). The proposed prototype is $5\lambda_0$ long having 10 unit cells. The beam scanning range of the proposed antenna is 107° within 9-13.5 GHz, maximum broadside radiation efficiency of ∼96%.**

***Index Terms*—Substrate integrated waveguide, Composite right/left handed (CRLH), Leaky-wave antenna.**

I. Introduction

COMPOSITE right/left handed (CRLH) transmission-lines (TLs) represent an artificially structured media having unique properties which have been used extensively in several applications over the past decades [1]. Besides this, with the rapid growth of wireless technology, the demand of improved antenna performances like high gain, larger scanning range etc. are highly needed in various surveillance systems and many scanning applications. Leaky-wave antenna (LWA) appears to be an appropriate choice for such applications which belongs to a traveling wave antenna family and has the capability of frequency beam scanning [2]. Recently, several compact leaky-wave antennas based on microstrip as well as on substrate integrated waveguide (SIW) environment open a new avenue for frequency-scanning antenna design [3]-[5].

Usually, the microstrip and waveguide based LWAs restrict the broadside radiation except the periodic LWAs having spatial harmonic and complex feeding network. Balanced CRLH TLs are one of the best choices to achieve broadside radiation which is capable to eliminate the open-stopband between the left-handed and right-handed regions. In past, several CRLH based LWAs have been developed for backfire to endfire radiation including broadside [6],[7]. Over the last few years the use of half-mode substrate integrated waveguide (HMSIW) and quarter-mode substrate integrated waveguide (QMSIW) in designing compact antennas as well as frequency beam scanning antennas have also increased extensively [8]-[12]. However, it is very difficult to achieve higher efficiency at broadside frequency, a constant high gain over the full operating frequency band maintaining a fair scanning range, design simplicity and compactness. In [13] and [14], new technique of efficiency enhancement at broadside frequency (η_{f_0}) has been proposed by using transversal asymmetry (TA) and double asymmetry (DA), respectively. However, both these designs suffer from drawbacks like larger electrical size, lower gain and higher cross-polar level. In this work a novel DA radiating structure by integrating it with the interdigital capacitive (IDC) slots has been proposed, which results into improved gain and higher efficiency as compared to those of earlier proposed simple DA structures [14]. It is to be noted that although the simple SIW based LWAs having interdigital capacitive slots have recently been proposed in literature [6], [16-20], but most of these designs either have larger electrical size or lesser beam scanning range with the typical maximum radiation efficiency of lesser than 80%. Hence, it can be inferred that the proposed IDC slot integrated DA radiating structures resulting into higher overall gain, improved efficiency and compact geometry are quite novel which have not been presented earlier in literature.

In this paper, an electrically small EMSIW resonator incorporated with interdigital slot is designed for the realization of compact high gain DA CRLH leaky-wave antenna for full space scanning through broadside with increased broadside radiation efficiency. The proposed design provides much easier independent control over series and shunt resonators by tuning the tilt angle of the IDC slot (θ) and the EMSIW resonator (ζ), respectively to achieve the balanced condition. This further helps to tune the transformation ratio (T) and enhances the η_{f_0} notably. The performance of the proposed antenna is optimized using HFSS and validated by experiments. Due to the appropriate placement of IDC slots on the top of the radiating EMSIW resonator, the radiation intensity profile, gain and η_{f_0} are improved without significantly increasing the length. The scanning angle can be varied from -64° to +43° by varying frequency from 9-13.5 GHz with the radiator length of $5\lambda_0$.

II. Proposed Double Asymmetry CRLH Unit Cell and Circuit Analysis

Firstly, the eighth mode SIW is developed where a square SIW resonator is divided across the perfect open symmetry plane (fictitious magnetic wall) [15]. The EMSIW unit cell is slightly tilted at an angle ζ with proper feeding line position which controls the radiation characteristic as well as scanning range of the antenna. The normalized phase constant and attenuation constant are optimized with ζ=21°, m_1=2.36 mm, L_1=8.51 mm, m_2=2.32 mm, d=0.8 mm and s=1.2 mm. IDC slots are etched on the top of the radiating tilted EMSIW resonator to realize the novel composite right/left handed media (Fig. 1(a)) which exhibits a larger radiation intensity compared to the simple EMSIW or conventional series fed patch based LWA [14] as depicted in Fig. 2(a). Hence, this proposed unit cell provides higher directivity and gain. The radiation intensity in a particular direction is straightway defined as the radiated power from a radiating structure per unit solid angle. However, in HFSS simulator, the radiation intensity of the proposed unit cell is determined as $U(\theta,\phi)$ = $(|E|^2r^2)/2\eta_0$ where, $|E|$ is the magnitude of the E-field, η_0 is the intrinsic impedance in free space (376.7 ohm) and r is the distance from antenna in meters. Moreover, the CRLH unit cell exhibits DA with respect to transverse as well as longitudinal axis as shown in Fig. 1(b) where the independent control over series and

A. Sarkar, A. Sharma, A. Biswas and M. Jaleel Akhtar are with the Department of Electrical Engineering, Indian Institute of Technology Kanpur, Kanpur, UP, 208016, India (e-mail: anirban.skr227@gmail.com).

This article has been accepted for publication in a future issue of this journal, but has not been fully edited. Content may change prior to final publication. Citation information: DOI 10.1109/TAP.2019.2918443, IEEE Transactions on Antennas and Propagation

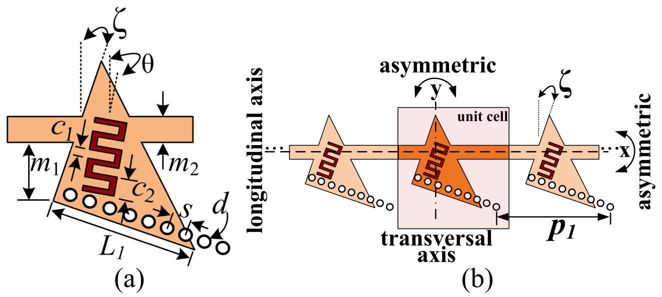

Fig. 1. (a) Proposed unit cell, (b) Layout of proposed CRLH based DA balanced LWA.

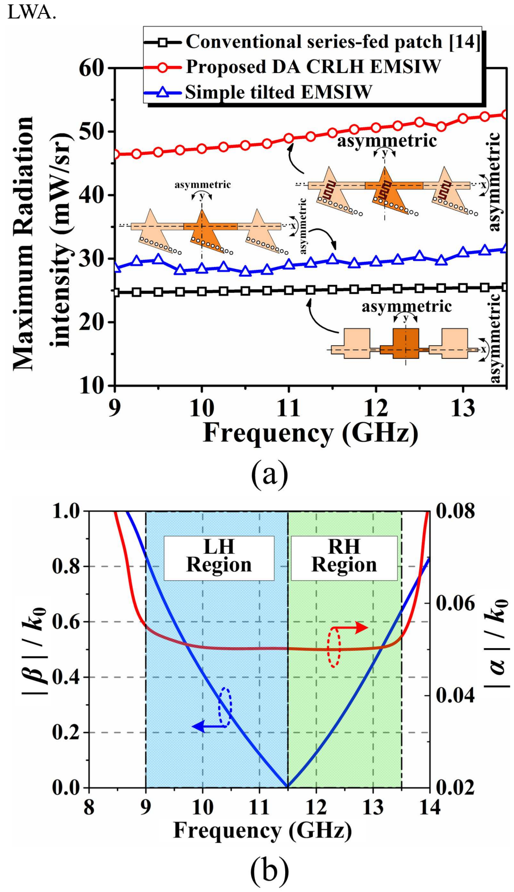

Fig. 2. (a) Comparison of radiation intensity per unit cell for conventional and proposed design, (b) Dispersion diagram of the balanced unit cell with c_1=0.26 mm c_2=0.84 mm.

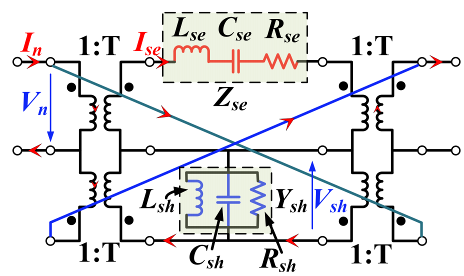

Fig. 3. Equivalent lattice circuit model of the proposed LWA unit cell.

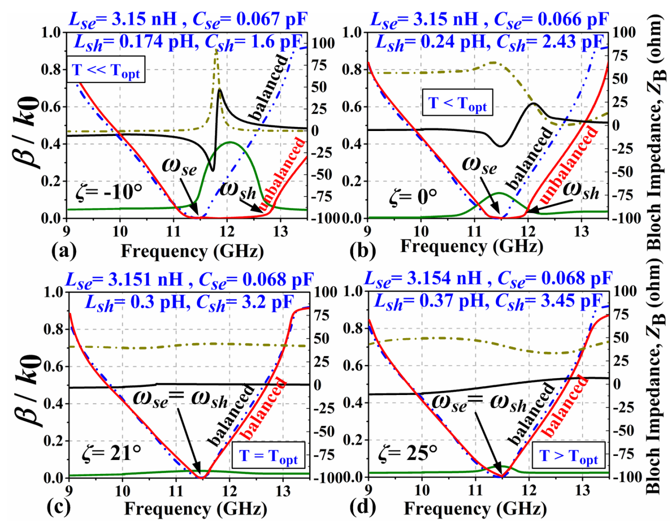

Fig. 4. Variation of ζ and its effect on dispersion diagram for (a) $T \ll T_{opt}$, (b) $T < T_{opt}$, (c) $T = T_{opt}$ and (d) $T > T_{opt}$.

shunt resonators of the proposed unit cell to tune the transformation ratio is predominantly an unique feature of the proposed antenna to enhance the efficiency at broadside frequency. Basically, due to the use of interdigital slot on radiating EMSIW causes higher radiation loss per unit cell. Hence, the condition for $\sim 90\%$ of total power will be radiated into space, is fulfilled with the much compact radiator length of $5\lambda_0$. To the author's best knowledge, this feature is not utilized so far in the available literature. In full-wave optimization of unit-cell analysis, isolation of the series mode with PEC boundaries and shunt mode with PMC boundaries are achieved from where the series resonance frequency (f_{se}), the series radiation efficiency (η_{se}), the shunt resonance frequency (f_{sh}) and the shunt radiation efficiency (η_{sh}) are calculated [14].

A. Technique 1: Enhancement of η_{f_0} by independent shunt parameter control equivalently varying EMSIW resonator tilt angle (ζ)

The equivalent circuit model of the proposed unit cell can be obtained by dividing the unit cell into the series and shunt resonators along with four coupling transformers having transformation ratio 1:T which control the coupling of power ratios between series and shunt resonator. The input and output coupling sections are represented by two transformers having the transformation ratio 1:T as shown in Fig. 3. The series resonance is comprised of series inductance (L_{se}) and series capacitance (C_{se}) which are due to the presence of the top wall of the tilted EMSIW resonator and the tilted IDC slot, respectively. The shunt resonance is comprised of shunt inductance (L_{sh}) and shunt capacitance (C_{sh}) which are due to metallic vias and ground plane-tilted EMSIW resonator top surface, respectively. The parameter T can be physically interpreted as additional variable which can be changed by varying tilt angle of EMSIW resonator (ζ). The equivalent circuit lattice model of the unit cell is shown below in Fig. 3. The circuit simulations are performed in ADS. Primarily, f_{se} and f_{sh} are calculated by imposing the odd excitation with $Im\{Z_{se}\}\,|_{f_{se}} = 0$ and even excitation with $Im\{Y_{sh}\}\,|_{f_{sh}} = 0$ respectively. If we vary the EMSIW resonator tilt angle ζ, the affected parameters are L_{sh} and C_{sh} which are due to the change of via positions and resonator positions, respectively. Hence, the change of resonator tilt angle only affects the total shunt admittance Y_{sh}. With the increase of tilt angles, the shunt resonance frequency is solely moving towards the desired balanced frequency 11.5 GHz keeping the series resonance frequency almost stationary. The increment of L_{sh} with increment of resonator tilt angle ζ is not significant as number of vias is not changing. Whereas, increment of C_{sh} is more prominent due to the changing position of EMSIW. The increment of C_{sh} implies the increment of shunt admittance which increases the shunt contribution in radiation mechanism. In the full wave simulation of unit cell, wave-port excitation is carried out. By considering the effect of periodicity, the unit cell is simulated in HFSS and the S-

This article has been accepted for publication in a future issue of this journal, but has not been fully edited. Content may change prior to final publication. Citation information: DOI 10.1109/TAP.2019.2918443, IEEE Transactions on Antennas and Propagation

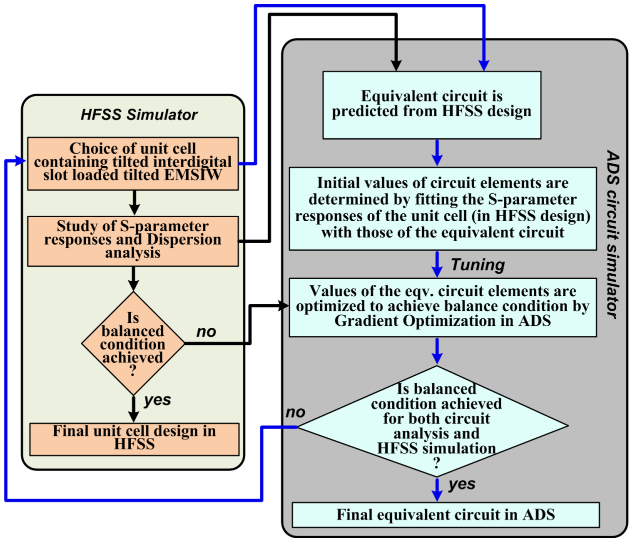

Fig. 5. Block diagram of the optimization procedure, performed by coupling the circuit simulator, ADS with full-wave simulator, Ansys HFSS.

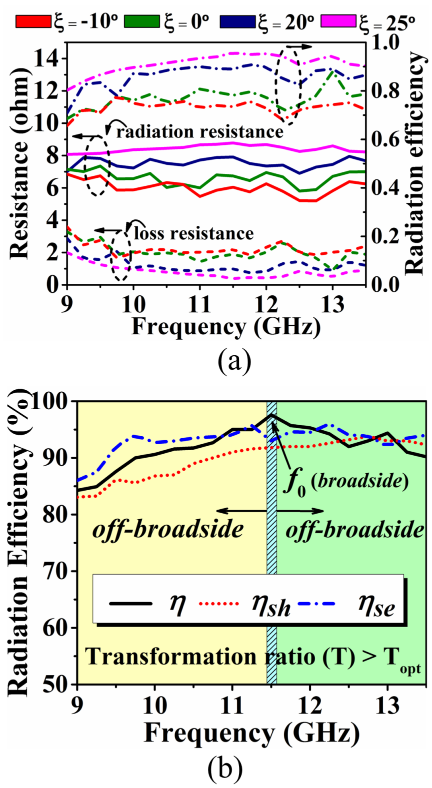

Fig. 6. (a) Variation of EMSIW resonator tilt angle ζ and its effect on radiation resistance, loss resistances and efficiency, (b) Variation of series, shunt and overall radiation efficiency of the proposed antenna.

parameters are extracted to study the dispersion characteristics. The dispersion equation of the periodic TL can be extracted from full-wave simulations [4],[5]. The dispersion curve of the proposed unit cell in the present situation is obtained by computing the β and α parameters using the following expression:

$$\beta = \frac{1}{p_1}\left|\mathrm{Im}\left(\cosh^{-1}\left(\frac{1 - S_{11}S_{22} + S_{12}S_{21}}{2S_{21}}\right)\right)\right| \tag{1}$$

$$\alpha = \frac{1}{p_1}\left|\mathrm{Re}\left(\cosh^{-1}\left(\frac{1 - S_{11}S_{22} + S_{12}S_{21}}{2S_{21}}\right)\right)\right| \tag{2}$$

where, the HFSS full wave simulator is employed to estimate the S-parameters of the cell in terms of its geometry at specified frequency points. After estimating the β and α parameters, the dispersion diagram representing the factors ($\mid \beta \mid /k_0$) and ($\mid \alpha \mid /k_0$) with $k_0 = 2\pi f/c$ as a function of frequency f is plotted as shown in Fig. 2(b). It is observed from the dispersion diagram (Fig. 2(b)) that at the transition frequency (f_0=11.5 GHz) where radiated fan-beam is in broadside direction, f_{se} and f_{sh} are equal. Thus, balance condition is achieved. At this condition, phase constant β exhibits zero value at the transition frequency. Below this frequency, the LH region appears which supports the propagation of backward-wave and just above the transition frequency is RH region which supports forward-wave. After achieving the balanced condition, if we now increase the resonator tilt angle furthermore which signifies the excessive asymmetry, the shunt capacitance further increases and transformation ratio exceeds its optimal value. Basically, the variation of tilt angle (ζ) is a very easier way to get excessive asymmetry in transverse as well as longitudinal direction. The proposed asymmetry gradually decreases the shunt Q-factor to a value of $\sim$ 12.72, which eventually enhances the shunt radiation contribution. Similarly, the series Q-factor is also enhanced during this process resulting into the value of 12.73. At this condition, η_{f_0} enhances from off-broadside. η_{f_0} is the overall radiation efficiency at broadside frequency (f_0) i.e. 11.5 GHz and it can be calculated from [14]. The variation of ζ and its effect on dispersion diagram and bloch impedance (Z_B) are shown in Fig. 4 where the optimized circuit element values are mentioned for each steps. The detailed methodology to design the equivalent circuit model in ADS from full-wave simulation is shown in Fig. 5 by flow chart. Moreover, one can justify if the tilt angle ζ increases, the radiation resistance R_{rad} also increases because of larger accumulation of charges at the tip of the resonator along with decrements of loss resistance. As a result overall radiation efficiency increases and after $\zeta > \zeta_{opt}$ value (ζ = 25°) (Fig. 4(d)), even it is greater than off-broadside because of the excessive shunt coupled power transfer to load as shown below in Fig. 6(a).

B. Technique 2: Enhancement of η_{f_0} by independent series parameter control equivalently varying the tilt angle of IDC slot (θ)

The proposed design provides another way to control the transformation ratio and hence to improve the broadside radiation efficiency profile. In this approach, even and odd excitation analysis are carried out in a similar manner as mentioned in the previous approach. For this situation, the tilt angle of the IDC slot (θ) is varied. The IDC slot mostly affects the series capacitance C_{se}, but variation of θ also change L_{se}. When the IDC slot tilt angle θ increases gradually, the series inductance and capacitance both are decreased. As a result, the series resonance frequency is moved towards higher value. For the θ of 10°, both the series and shunt frequencies are equal and fulfill the balanced condition at 11.5 GHz. At this point, transformation ratio reaches its optimal value (T = 1.079) and the Q-factor for series and shunt resonances are equal and it is obtained as 12.73. Here, the η_{f_0} is almost equal to the off-broadside and the series and shunt modes are no longer exist because of by forming new coupled modes. Now if one increases θ more than 10° (13° for our design purpose), i.e. asymmetry is applied beyond the optimal point, the C_{se} and L_{se} are also decreased furthermore keeping the dispersion behavior almost unchanged. Thus, series impedance increases with increased V_{se}/I_{se}. Parallely, due to the simultaneous increment of increased series radiation resistance, series power ratio is enhanced with maximum coupling of series power. The above described detailed analysis shows that the overall radiation efficiency at broadside direction (η_{f_0}) has been increased by controlling the power ratio between the series

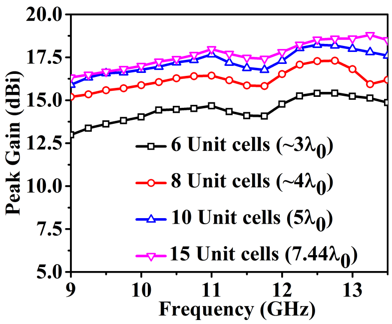

Fig. 7. Selection of compact antenna size by optimizing peak gain variation for different radiator lengths.

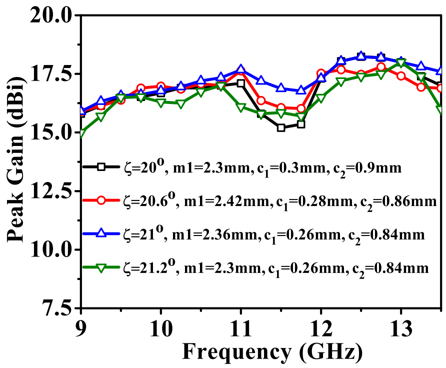

Fig. 8. Gradual optimization for the selection of structural parameters to minimize the gain drop in broadside direction.

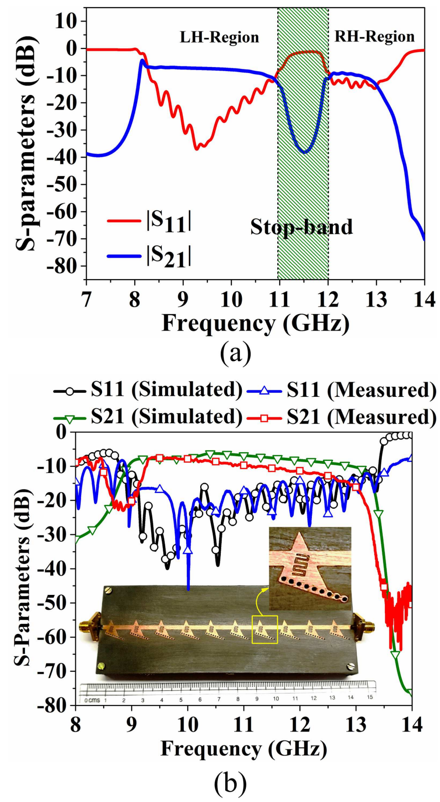

Fig. 9. S-parameter responses of the (a) unbalanced CRLH leaky-wave antenna with broadside null, (b) proposed balanced CRLH leaky-wave antenna.

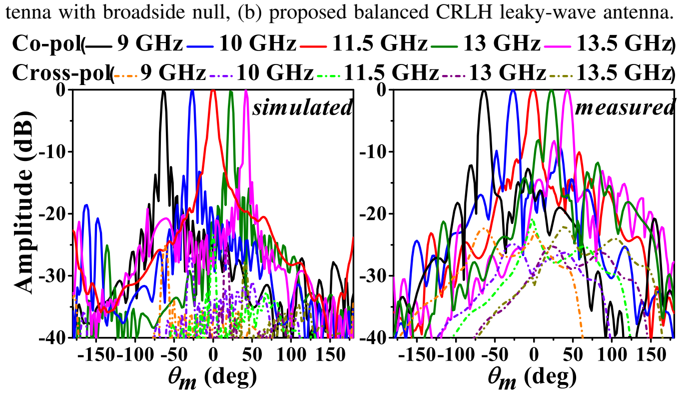

Fig. 10. (a) Simulated and (b) measured radiation patterns of the proposed leaky-wave antenna in x-z plane at 9 GHz (θ_m= -60°), 10 GHz (θ_m= -25°), 11.5 GHz (θ_m= 0°), 13 GHz (θ_m= 23°), 13.5 GHz (θ_m= 40°).

and the shunt resonators through larger transversal asymmetry. The series and shunt radiation efficiency are calculated from [14]. The efficiency at broadside frequency (η_{f_0})of ($\sim$ 96%) is achieved over off-broadside and is shown in Fig. 6(b).

III. Leaky-wave Antenna Design

The balanced CRLH unit cell shown in Fig. 1(a) is placed periodically in series with the periodicity p_1 (maintaining the homogeneity condition i.e. $p_1 \ll \lambda_g/4$) in such a manner that the scanning range of the leaky-wave antenna will be in the fast wave region (9-13.5 GHz) where n^{th} space harmonic phase constant (β_n) increases from negative (β_n = -k_0) to positive (β_n = k_0) values with increment of frequencies. In the fast wave region, β_n is less than the free space wave number i.e. $\mid \beta_n \mid < k_0$ which is necessary radiation condition of LWA. In the proposed design, n = 0 harmonic is responsible for radiation and it is termed as β. According to the Hensen Woodyard maximum directivity condition [2], the largest directivity of our proposed antenna will occur for the radiator length of 133 mm ($5\lambda_0$) which contains 10 unit cells. If we increase the radiator length i.e increase the number of unit cells, the gain is increased accordingly but it doesn't shows significant improvement after $5\lambda_0$. Little increment is observed due to slight improvement of the radiation efficiency. Selection of compact antenna size by optimizing peak gain variation for different radiator lengths is shown in Fig. 7 from where it is clear that maximum directivity and gain can be achieved with radiator length of $5\lambda_0$ keeping the antenna size most compact. It is also observed that the inaccurate dispersion is responsible for gain degradation in broadside direction. In order to minimize the gain drop along the broadside direction, the precise tuning of various structural parameters of the proposed unit cell structure is carried out in the gradual fashion. The optimization results into minimum gain drop around the broadside frequency point as shown by blue line in Fig. 8. The angle of radiation from z-axis can be determined from (3)[21]

$$\theta_m = \sin^{-1}\left(\frac{\mid \beta \mid}{k_0}\right) = \sin^{-1}\left(\frac{\mid \beta \mid \cdot c}{2\pi f}\right) \tag{3}$$

IV. Results and Discussion

To validate the proposed design experimentally, the prototype is fabricated on Rogers RT/duroid 5880 substrate having the dielectric constant (ϵ_r) of 2.2, loss tangent (tanδ) of 0.0009 and thickness (t) of 0.787 mm. The fabricated prototype is shown in Fig. 9(b). The simulated and measured 10 dB return loss bandwidth (Fig. 9(b)) of the proposed antenna are achieved of 40.64% (8.88-13.41 GHz) and 40.89% (8.93-13.52 GHz) respectively. The open stop-band shown in Fig. 9(a) (broadside null at 11.5 GHz), is successfully suppressed and as a result, broadside radiation is obtained. The simulated and measured normalized radiation patterns are depicted in Fig. 10(a) and (b) where the measured radiated beam of the proposed antenna

TABLE I
PERFORMANCE COMPARISON OF PROPOSED STRUCTURE WITH OUR SIMPLE EMSIW BASED LWA

Unit cell configuration	Length	Deg. of freedom	η_{f0}	BW	G_p (dBi)	$\Delta\theta$
Simple EMSIW based LWA	$7.26\lambda_0$ with 10 unit cells	Limited	90.8%; (limited η_{f0} because equalization of η_{se} and η_{sh} limit η_{f0} up to certain point)	22.22% (8-10 GHz)	13.31 dBi (simple EMSIW has lower radiation intensity)	Only 1 quadrant scanning of 51° (37° to 88°)
Proposed DA EMSIW based CRLH LWA with tilted IDC	**$5\lambda_0$ with 10 unit cells; more compact**	**Larger**	**96%; (independent control over η_{se} and η_{sh} enhance η_{f0} significantly)**	**40.89% (9-13.5 GHz)**	**17.96 dBi (high gain and directivity due to larger radiation intensity)**	**Full space 2 quadrant scanning of 107° (-64° to +43°)**

TABLE II
PERFORMANCE COMPARISON WITH OTHER REPORTED DESIGNS

Reference	Length	Bandwidth (%)	G_p (dBi)	$\Delta\theta$	η_{f0}
[6] SIW based CRLH LWA	$7\lambda_0$	8.6-12.8 GHz(39.25%)	10.8	130°	78%
[7] CRLH based Multilayer LWA	$12.95\lambda_0$	20-30 GHz(40%)	14	75°	54%
[9] HMSIW based CRLH LWA	$4.85\lambda_0$	13.5-17.8 GHz(27.47%)	16	86°	83%
[12] HMSIW based LWA	$6.6\lambda_0$	9-13.5 GHz(30.3%)	10	86°	64%
[13] Series-fed patch based TA P-LWA	$27\lambda_0$	9-11 GHz(20%)	NA	NA	69%
[14] Series-fed patch based DA P-LWA	$\sim 5\lambda_0$	22-26 GHz(16.6%)	8.5	NA	86%
EMSIW based LWA without IDC	$\sim 5.2\lambda_0$	8-10 GHz(22.22%)	13.31	51°	84%
Proposed: EMSIW based CRLH DA LWA	**$5\lambda_0$**	**9-13.5 GHz(40.89%)**	**17.96**	**107°**	**96%**

η_{f0} = radiation efficiency at broadside frequency.

TABLE III
PERFORMANCE COMPARISON WITH OTHER IDC SLOT BASED REPORTED DESIGNS

Design of CRLH based LWAs with IDC unit cell	Radiator length	Bandwidth(%)	G_p (dBi)	$\Delta\theta$	η_{MAX}
[6] SIW based CRLH LWA with IDC slots 	$7\lambda_0$	8.6-12.8 GHz(39.25%)	10.8	130° (-70° to +60°)	78%
[16] SI CRLH LWA with orthogonal IDC pair 	$5.6\lambda_0$	7.5-10 GHz(25.57%)	12	80° (-30° to +40°)	80%
[17] IDC loaded HMSIW based LWA 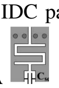	$3.25\lambda_0$	Fixed freq. beam scanning	~ 10	67° (-31° to +35°)	NA
[18] HMSIW based LWA with ramp-shaped IDC 	$6.2\lambda_0$	7.4-13.5 GHz(54%)	12.01	140°(-70° to +70°	NA
[19] SIW based CRLH LWA with ±45° tilted IDC 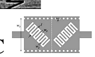	$2.42\lambda_0$	4.2-4.85 GHz(14.36%)	2.5	51° (-25° to +26°)	NA
[20] SIW based CRLH LWA with T-shaped IDC pair 	$5.6\lambda_0$	7.15-10.35 GHz(36.57%)	8.95	103° (-19° to +84°)	69%
Proposed: EMSIW based CRLH LWA with tilted IDC 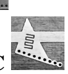	$5\lambda_0$	**9-13.5 GHz(40.89%)**	**17.96**	**107° (-64° to +43°)**	**96%**

G_p = Peak gain, $\Delta\theta$ = Scanning range, η_{MAX} = maximum radiation efficiency.

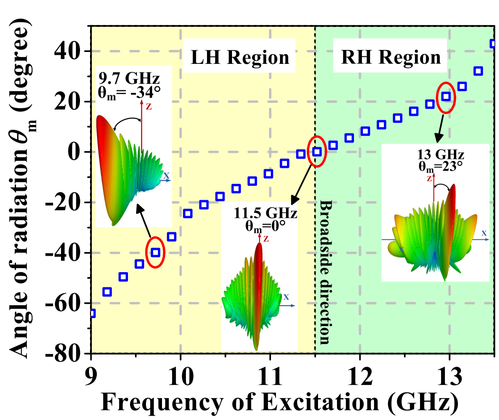

Fig. 11. Variation of angle of radiation with excitation frequency (3D patterns are in inset for three different frequencies).

scans from the left handed region of θ_m= -64° at 9 GHz to right handed region of θ_m= 43° at 13.5 GHz including broadside radiation at 11.5 GHz. The measured scanning range is obtained as 107°. Little discrepancy in measured radiation pattern is due to larger leakage loss resulting larger beamwidth. The measured minimum cross-polarization levels are obtained as -22.39 dB at 9GHz, -24.89 dB at 10 GHz, -20.74 dB at 11.5 GHz, -22.16 dB at 13 GHz and -25.29 dB at 13.5 GHz. Now, in order to estimate the angle of radiation (θ_m) as a function of frequency using (3), the phase constant (β) in terms of S-parameters of the corresponding unit cell along with its periodic length (p_1) is obtained using the data given in Fig. 2(b). Once, the factor ($\mid \beta \mid /k_0$) is determined using the data given in Fig. 2(b), the curve showing the plot of the angle of radiation θ_m (in the vertical axis) versus the corresponding frequency of excitation 'f' (in horizontal axis) can be obtained using equation (3) as shown in Fig. 11. Fig. 12 demonstrates that the peak gain (G_p) and overall radiation efficiency values obtained from simulation and measurement, are in good agreement. In order to show the advantages of the proposed antenna, a detailed comparison is made with our own simple EMSIW based structure as well as with similar types of structures proposed in literature as shown in Table I and

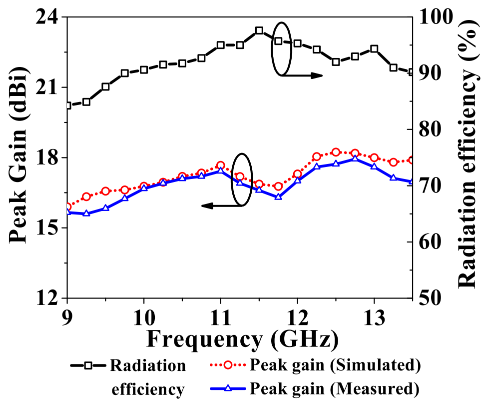

Fig. 12. Variation of peak gain and overall radiation efficiency with frequency.

II, respectively. The proposed prototype appears to be a much better alternative as compared to the simple EMSIW based LWA to facilitate wider scanning range, higher gain and larger radiation efficiency with much compact geometry. Owing to the incorporation of suitably tilted IDC slot on tilted EMSIW, not only larger degrees of freedom is achieved to independently control series and shunt parameters but also increase in the radiation intensity results in significant gain enhancement and compactness. It can clearly be seen from Table II that the proposed antenna is advantageous in terms of high gain, enhanced efficiency at broadside frequency with additional degrees of freedom, compact size and good operating bandwidth along with suitable scanning range than other reported designs. It is to be noted that, [6], [7], [9], [12] and [13] have considerably low η_{f_0} due to either double symmetry or single asymmetry. Although [14] has double asymmetry with comparable size and therefore increased η_{f_0}, but suffers lower G_p (8.5 dBi), inadequate bandwidth (16.6%), lesser radiation efficiency (86%) at broadside frequency and higher cross-polar level of -13.75 dB compared to the proposed design. To analyze the proposed LWA performance rigorously, the proposed structure with optimized IDC configuration is compared with earlier reported CRLH based IDC loaded leaky-wave antenna structures as shown in Table III. In Table III, although [16] and [20] have almost comparable radiator lengths, but the proposed structure is advantageous in terms of higher gain, larger radiation efficiency and working bandwidth. It should be noted although the work proposed in [6] and [18] of Table III provide larger scanning ranges along with comparable operating bandwidth, but the proposed structure is advantageous due to its higher gain, much compact dimension and larger radiation efficiency.

V. Conclusion

A simple high gain larger full space scanning range compact LWA based on the use of double asymmetry CRLH unit cell has been demonstrated. The proposed structure makes use of the tilted radiating EMSIW incorporated with interdigital capacitive slot to realize CRLH media which enhances the radiation intensity profile of the unit cell significantly resulting higher directivity and gain keeping the proposed prototype quite compact. Maintaining the frequency balanced condition of our proposed unit cell, the propagation constant and Bloch impedance of the series and shunt resonators can be independently controlled for easier tuning of transformation ratio to obtain larger efficiency at broadside frequency over off-broadside and it is achieved of $\sim$96%. The proposed antenna shows a fair scanning range of 107° (-64° to +43°) with a high gain of 17.96 dBi. The measured results are in well accordance with experiments which proves the effectiveness and validity of the proposed design. Having the advantages of more degrees of freedom to achieve larger efficiency, simple design methodology, being compact, adequate gain and larger scanning range, the proposed antenna could be the potential candidate for several frequency beam scanning applications.

References

[1] C. Caloz and T. Itoh, *Electromagnetic Metamaterials: Transmission Line Theory and Microwave Applications.* Hoboken, NJ: Wiley/IEEE, 2005.

[2] D. R. Jackson and A. A. Oliner, ‘Leaky-wave antennas’ in C. A. Balanis, ‘Modern Antenna Handbook’ (Ed. Hoboken, NJ, USA: Wiley, blue).

[3] S. T. Yang and H. Ling, “Two-section half-width microstrip leaky wave antenna,” *IEEE Trans. Antennas. and Propag.*, vol. 62, no. 10, pp. 4988-4996, Oct. 2014.

[4] J. Liu, D. R. Jackson, and Y. Long, “Substrate integrated waveguide (SIW) leaky-wave antenna with transverse slots,” in *IEEE Trans. Antennas Propag.*, vol. 60, no. 1, pp. 20-29, Jan. 2012.

[5] A. Sarkar, A. Sharma, M. Adhikary, A. Biswas and M.J. Akhtar, “Bidirectional SIW leaky-wave antenna using TE_{20} mode for frequency beam scanning,” in *Electronics Letters*, vol. 53, no. 15, 1017-1019, July 2017

[6] Y. Dong and T. Itoh, “Composite right/left-handed substrate integrated waveguide and half mode substrate integrated waveguide leaky-wave structures,” in *IEEE Trans. Antennas Propag.*, vol. 59, no. 3, pp. 767-775, Mar. 2011.

[7] W. Jiang, C. Liu, B. Zhang and W. Menzel, “K-band frequency-scanned leakywave antenna based on composite right/left-handed transmission lines,” *IEEE Antennas Wireless Propag. Lett.*, vol. 12, pp. 1133-1136, 2013.

[8] J. Xu, W. Hong, H. Tang, Z. Kuai and K. Wu, “Half-mode substrate integrated waveguide (HMSIW) leaky-wave antenna for millimeterwave applications,” *IEEE Antennas Wireless Propag. Lett.,* vol. 7, pp. 85-88, 2008.

[9] A. Sarkar, M. Adhikary, A. Sharma, A. Biswas, M. J. Akhtar and Z. Hu, “Composite right/left-handed based compact and high gain leaky-wave antenna using complementary spiral resonator on HMSIW for Ku band applications,” in *IET Microw. Antennas Propag.*, vol. 12, no. 8, pp. 1310-1315, July 2018.

[10] D. Lee and S. Lim, “Leaky-wave antenna design using quarter-mode substrate-integrated waveguide,” *Microwave Opt. Technol. Lett.,* 57 (2015), 1234-1236.

[11] M. U. Memon and S. Lim, “Frequency-tunable compact antenna using quarter-mode substrate integrated waveguide,” in *IEEE Antennas Wireless Propag. Lett.*, vol. 14, pp. 1606-1609, 2015.

[12] R. Henry and M. Okoniewski, “A broadside-scanning half-mode substrate integrated waveguide periodic leaky-wave antenna,” in *IEEE Antennas Wireless Propag. Lett.,*, vol. 13, pp. 1429-1432, 2014.

[13] S. Otto, A. Al-Bassam, A. Rennings, K. Solbach, C. Caloz, “Transversal asymmetry in periodic leaky-wave antennas for bloch impedance and radiation efficiency equalization through broadside,” *IEEE Trans. Antennas and Propag.,* vol. 62, no. 10, pp. 5037-5054, July. 2014.

[14] A. Al-Bassam, S. Otto, D. Heberling, C. Caloz, “Broadside dual-channel orthogonal-polarization radiation using a double-asymmetric periodic leaky-wave antenna,” *IEEE Trans. Antennas and Propag.,* vol. 65, no. 6, pp. 2855-2864, June. 2017.

[15] S. Sam and S. Lim, “Electrically small eighth-mode substrate-integrated waveguide (EMSIW) antenna with different resonant frequencies depending on rotation of complementary split ring resonator,” *IEEE Trans. Antennas and Propag.,* vol. 61, no. 10, pp. 4933-4939, 2013.

[16] Y. D. Dong and T. Itoh, “Substrate integrated composite right-/left handed leaky-wave structure for polarization-flexible antenna application,” *IEEE Trans. Antennas and Propag.,* vol. 60, no. 2, pp. 760-771, Feb. 2012.

[17] A. Suntives and S. V. Hum, “A Fixed-Frequency Beam-Steerable Half-Mode Substrate Integrated Waveguide Leaky-Wave Antenna,” *IEEE Trans. Antennas and Propag.,* vol. 60, no. 5, pp. 2540-2544, May. 2012.

[18] A. P. Saghati, M. M. Mirsalehi and M. H. Neshati, “A HMSIW Circularly Polarized Leaky-Wave Antenna With Backward, Broadside, and Forward Radiation,” *IEEE Antennas Wireless Propag. Lett.,* vol. 13, pp. 451-454, 2014.

[19] H. Lee, J. H. Choi, C. M. Wu and T. Itoh, “A Compact Single Radiator CRLH-Inspired Circularly Polarized Leaky-Wave Antenna Based on Substrate-Integrated Waveguide,” *IEEE Trans. Antennas and Propag.,* vol. 63, no. 10, pp. 4566-4572, Oct. 2015.

[20] M. M. Sabahi, A. A. Heidari and M. Movahhedi, “A Compact CRLH Circularly Polarized Leaky-Wave Antenna Based on Substrate-Integrated Waveguide,” *IEEE Trans. Antennas and Propag.,* vol. 66, no. 9, pp. 4407-4414, Sept. 2018.

[21] C. A. Balanis, *Modern Antenna Handbook*. New York: Wiley, 2008.